Kondo Interactions and Magnetic Correlations in $CePt_2$ Nanocrystals

Y. Y. Chen,[1,*] P. H. Huang,[1] M. N. Ou,[1,2] C. R. Wang,[3] Y. D. Yao,[1,†] T. K. Lee,[1] M. Y. Ho,[1] J. M. Lawrence,[4] and C. H. Booth[5]

[1]*Institute of Physics, Academia Sinica, Taipei, Taiwan, Republic of China*
[2]*Department of Electrophysics, National Chiao Tung University, Hsinchu, Taiwan, Republic of China*
[3]*Department of Physics, Tunghai University, Taichung, Taiwan, Republic of China*
[4]*Department of Physics and Astronomy, University of California, Irvine, California 92697 USA*
[5]*Chemical Sciences Division, Lawrence Berkeley National Laboratory, Berkeley, California 94720 USA*

(Received 7 December 2006; published 13 April 2007)

The evolution of the Kondo effect and antiferromagnetic (AF) correlations with size reduction in $CePt_2$ nanoparticles (3.1–26 nm) is studied by analysis of the temperature-dependent specific heat and magnetic susceptibility. The AF correlations diminish with size reduction. The Kondo effect predominates at small particle size with trivalent, small Kondo temperature (T_K) magnetic regions coexisting with strongly mixed-valent, large T_K nonmagnetic regions. We discuss the role of structural disorder, background density of states and the electronic quantum size effect on the results.

DOI: 10.1103/PhysRevLett.98.157206 PACS numbers: 75.30.Mb, 72.15.Qm, 75.40.Cx

In metals, the conduction band splits into discrete energy levels when the particle size is reduced to the nanoscale [1]. For a Kondo system, when the mean electronic level spacing ξ becomes comparable or larger than the Kondo temperature T_K and/or the magnetic ordering temperature T_N, the physical properties should be altered. The Kondo effect generated by a single magnetic impurity in nanostructures and organometallic molecules has been investigated both theoretically [2,3] and experimentally [4–6]. Nanostructures of Kondo *lattice* compounds, however, have rarely been investigated. In such materials both the Kondo effect and the Rudermann-Kittel-Kasuya-Yosida (RKKY) interaction need be taken into account [7]. Measurements of x-ray absorption fine-structure (XAFS) on $CeAl_2$ nanoparticles showed that structural disorder in the nanoparticles also plays a role in the behavior [8]. Theoretical work on Kondo lattice nanoclusters alloyed with mixed-valent impurities showed that the local Kondo temperature T_K and RKKY interactions are strongly enhanced by disorder [9]. Experimentally, the size dependence of the Kondo temperature T_K has been found to be different in different systems [7,10].

Here we report measurements of the specific heat $C(T)$ and susceptibility $\chi(T)$ of a series of specimens of the Kondo lattice compound $CePt_2$ as the particle size decreases to nanoscale. $CePt_2$ grows in the cubic $C15$ ($MgCu_2$) Laves phase. It is an antiferromagnet ($T_N = 1.7$ K) which is subject to cubic crystal-field splitting between a ground state Γ_7 doublet and an excited Γ_8 quartet of trivalent cerium ions [11,12]. The Kondo temperature is estimated to be of order 5 K [13].

The bulk $CePt_2$ was prepared by arc melting the constituent elements. Nanoparticles of 3.1 nm were fabricated by flash evaporation, whereas nanoparticles of $d = 22$ and 26 nm were grown by laser ablation. The x-ray diffraction of nanoparticles exhibited no change of structure relative to the bulk but did reveal an increase of linewidth characteristic of ultrasmall particles (Fig. 1). The lattice constants (Table I) were determined using Rietveld refinement; the average sizes of the nanoparticles were determined by the width of the diffraction peaks using the formula

$$\frac{\beta^2}{\tan^2\theta_0} = k\frac{\lambda}{L}\frac{\beta}{\tan\theta_0 \sin\theta_0} + 16e^2, \quad (1)$$

where β is the width (FWHM) of the diffraction line, θ_0 is the scattering angle, k is a constant, λ is the wavelength, L is the average particle diameter, and e is the strain along (h, k, l) [14]. The resulting particle sizes were further confirmed by high-resolution transmission electron microscopy (HRTEM) images (Fig. 1, photo inset). No noticeable oxidation was detected in the nanoparticles either by x-ray diffraction or HRTEM.

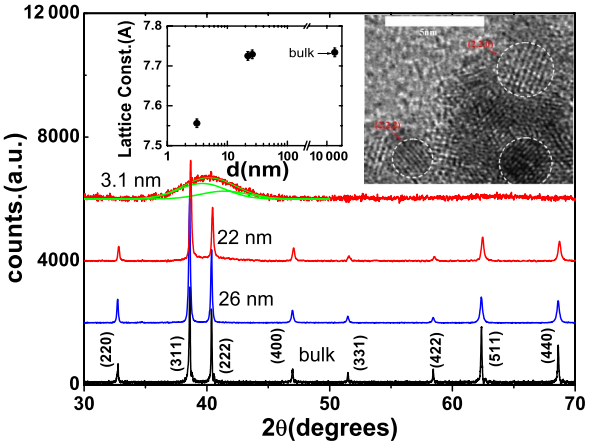

FIG. 1 (color online). X-ray diffraction patterns and Miller indices for bulk and nanoparticle $CePt_2$. Photo: HRTEM image of 3.8 nm $CePt_2$ reveals several well-crystallized particles in which (220) and (222) planes are indicated. Inset: the lattice constant vs diameter d.

TABLE I. The physical parameters obtained by fitting $C(T)$ and $\chi(T)$ for $CePt_2$ bulk and nanoparticles (see text for definitions).

Particle size (nm)	a_0(Å)	S_M (R ln2) or n_M	T_N (K)	n_{AF}	T_K (K)	n_K	n_K/n_M	Θ_D (K)	T_{cryst} (K)	C_{low} (emu/mol K)	C_{high} (emu/mol K)	C_{high}/C(Ce3+)
Bulk	7.731	1	1.6	0.4	5.6	0.6	0.6	200	110	0.37	0.79	0.98
26 ± 2	7.729	0.86	0.8	0.34	4.5	0.52	0.61	165	107	0.33	0.69	0.86
22 ± 2	7.725	0.69	0.7	0.22	4.1	0.47	0.68	150	100	0.25	0.45	0.56
3.1 ± 0.5	7.556	0.25	NA	NA	0.63	0.25	1	130	65	0.10	0.22	0.27

The temperature dependence of the specific heat of $CePt_2$ for the bulk and nanoparticles is shown in Fig. 2. The data for bulk $CePt_2$ is in good agreement with an earlier report [12]. A sharp peak near 1.6 K is superimposed on a low-temperature bump, reflecting the coexistence of magnetic correlations and Kondo interactions. For the 26 and 22 nm samples, there is a strong decrease in the amplitude of the low-temperature peak. As the size is further reduced to 3.1 nm no magnetic order is seen, but instead an upturn in the specific heat occurs below 2 K. To ascertain the origin of the upturn, further calorimetric measurements were made in external magnetic fields $H = 2$–8 T (Fig. 2, inset). If the upturn were caused by an antiferromagnetic transition, an applied field would lower the ordering temperature rather than increase it as observed. As can be seen from the inset to Fig. 2, the field dependence of the anomaly is qualitatively similar to the theoretical prediction [15] for a Kondo ion with $T_K = 0.63$ K.

As discussed further below, regions of the sample with essentially trivalent ''magnetic'' cerium, with small Kondo temperature, coexist with regions of strongly mixed-valent ''nonmagnetic'' cerium; the latter has a large T_K and makes a negligible contribution to the low-temperature specific heat. To extract detailed information from the total low-temperature specific heat C_{tot}, we need to account for the contributions C_{ph} from the lattice phonons, C_{cryst} from the crystal-field splitting, C_K from low-temperature Kondo interactions, and C_{AF} from the antiferromagnetic correlations. C_{ph} was determined by separate measurements on a nonmagnetic $LaPt_2$ counterpart. After phonon subtraction the crystal field T_{CF} is then estimated from the data (Fig. 3 and Table I). We label the low-temperature magnetic contribution as $C_M = C_{tot} - C_{ph} - C_{cryst} = C_K + C_{AF}$. For bulk $CePt_2$, the integrated entropy $S_M = \int (C_M/T) dT$ is close to 100% of R ln2 between 0 and 15 K. This result is consistent with a Γ_7 doublet ground state with $S = 1/2$ for trivalent cerium. Applying a similar analysis to the specific heat of the nanoparticles by taking the lattice phonon contribution from $LaPt_2$ nanoparticle counterparts, and defining the ''magnetic fraction'' as $n_M = S_M/R$ ln2, we find that $n_M = 0.86$, 0.69, and 0.25 for $d = 26$, 22, and 3.1 nm, respectively, (Table I). The remaining entropy $(1 - n_M)R$ ln2, presumably arising from regions of nonmagnetic, strongly mixed-valent cerium with a large T_K, is transferred to higher temperature.

The magnetic susceptibility $1/\chi$ versus T in the range 2–250 K for bulk and nanocrystalline $CePt_2$, shown in Fig. 4, confirms this decrease in the fraction of magnetic

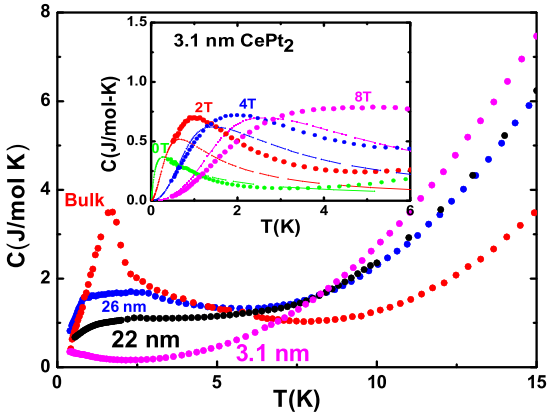

FIG. 2 (color online). $C(T)$ versus T for bulk and nanoparticle $CePt_2$. Inset: The solid circles represent the specific heat at various magnetic fields, the lines are the theoretical calculation.

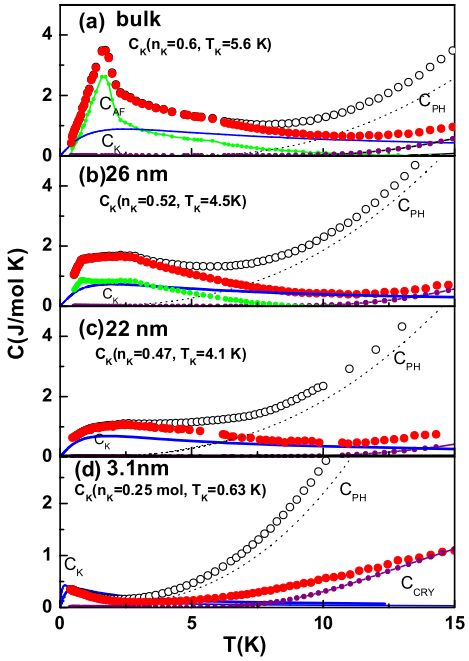

FIG. 3 (color online). The specific heat for (a) $CePt_2$ bulk (b) 26, (c) 22, and (d) 3.1 nm represented by open circles. The dashed lines represent the lattice phonon contribution C_{ph}; the solid circles represent the specific heat $C(T) - C_{ph}$; the solid lines represent the Kondo model fit C_K; and the dotted lines represent the crystal-field contribution C_{cryst}.

cerium. Except in the region 20–80 K where transitions begin to occur between the ground state Γ_7 doublet and the excited Γ_8 quartet [11,12], the susceptibility can be fit to a Curie-Weiss law $\chi(T) = C/(T - \Theta)$ at both high and low temperature. Here the Curie constant can be used to estimate the amount of trivalent cerium in the sample. For bulk $CePt_2$, the high-temperature (low-temperature) Curie constant $C_h(C_l)$ is observed to be 0.79(0.37) emu/K f.u.. Based on the theoretical value 0.807 emu K/f.u. for a free $J = 5/2$ moment, the high-temperature value indicates that the cerium atoms in bulk $CePt_2$ are ~100% trivalent. The negative Weiss temperature $\Theta_h \sim -39$ K obtained from the high-temperature region reflects demagnetization associated with the crystal-field splitting. For the nanoparticles, both C_h and C_l decrease with size reduction. The average percentages of magnetic cerium obtained from these Curie constants are ~85%, 61%, and 27% for 26, 22, and 3.1 nm, respectively, in good agreement with those obtained from the specific heat measurements (Table I).

While Kondo and antiferromagnetic interactions coexist in these materials and cannot be rigorously separated, Fig. 3 makes it clear that the AF contribution decreases dramatically as size decreases so that by 22 nm the behavior is very similar to that of an uncorrelated Kondo impurity. We can make a rough evaluation of the individual contributions $C_{\rm AF}$ and C_K to the total magnetic specific heat C_M as follows. We assume the contribution from magnetic correlations is negligible for $T > 10$ K. A first estimate of the Kondo contribution can then be extracted by fitting the data for $T > 10$ K to the theoretical Kondo specific heat C_K(theor) for 1 mol of $S = 1/2$ impurity [15]. After repeated iterations, tuning the parameters $T_{\rm cryst}$, T_K, and the fractional magnitude n_K of the Kondo contribution $C_K = n_K C_K$(theor), we achieve a best fit. The Néel temperatures were determined from the peak in the antiferromagnetic contribution $C_{\rm AF} = C_M - C_K$; the fractional magnitude $n_{\rm AF}$ of the AF contribution is defined via $n_{\rm AF} = \int (C_{\rm AF}/T) dT/R \ln 2 = n_M - n_K$. Given the rough approximation involved in separating the Kondo and AF contributions, these values are clearly only approximate, but adequately reflect the trends with particle size.

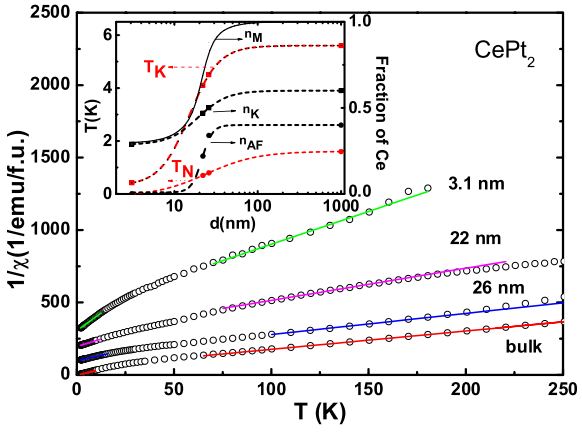

FIG. 4 (color online). The temperature dependence of the inverse susceptibility $1/\chi$ for bulk and nanoparticle $CePt_2$. The solid lines are Curie-Weiss fits. Inset: T_K and T_N (referred to the left axis) as well as the total fraction n_M of magnetic, trivalent cerium and the fraction Kondo and antiferromagnetic contributions n_K and $n_{\rm AF}$ (referred to the right axis) versus particle size d.

The results of the fitting are shown in Fig. 3 and the values of T_K, T_N, n_M, n_K, and $n_{\rm AF}$ are shown in Table I and the inset to Fig. 4, where they are plotted versus particle size. The results indicate that as size decreases from the bulk to 3.1 nm, the total amount n_M of magnetic cerium decreases, the relative fraction $n_{\rm AF}/n_M$ of the AF contribution decreases from 40% to zero, while the relative fraction n_K/n_M of the Kondo contribution increases from 60% to 100% (Table I).

While 25% of the 3.1 nm sample has a small Kondo temperature appropriate to trivalent cerium, the remaining 75% of the cerium is nonmagnetic. This fraction must arise from strongly mixed-valent cerium with a Kondo temperature sufficiently large (>1000 K) that it makes a negligible contribution to the specific heat ($C \sim 1/T_K$). Its presence can be deduced from the $L_{\rm III}$-edge XANES spectra of nanocrystalline $CePt_2$ [8] where the average $4f$ occupation number was found to be $n_f = 0.7$ for 3.8 nm $CePt_2$. This value could, for example, represent 75% of the cerium being strongly mixed valent with average f occupation $n_f = 0.6$ and 25% being trivalent ($n_f = 1$). Some of the strongly mixed-valent atoms occur as cerium oxide ($n_f = 0.5$); for example, for the 3.8 nm sample of Ref. [8], 15% of the cerium occurred as oxide. For the current sample, since there was no visible trace of oxide in the x-ray diffraction, this may be an overestimate.

The lattice constant (0.7717 nm) that we observe for 4 nm particles of the nonmagnetic, isostructural compound $LaPt_2$ is only 0.6% smaller than the value (0.7763 nm) we obtain for bulk $LaPt_2$. Hence we think that the larger (2.3%) lattice constant reduction observed in the 3.1 nm particles of $CePt_2$ (Table I) is not a normal consequence of small particle size. Rather, it is a typical consequence of mixed valence. Our measurements show that the linear coefficient of specific heat γ of $LaPt_2$ increases from 0.005 J/mol-K^2 in the bulk to 0.010 J/mol-K^2 for 4 nm particles. This doubling of the background density of states $N(0)$ can, when introduced into the exponential formula $T_K \sim \exp[-1/N(0)J]$, lead to a large increase in Kondo temperature and hence may explain the large increase in Kondo temperature and onset of strong mixed valence in most of the sample.

The spatial distribution of the different valence states is an open question. While it is not possible to precisely determine the ratio of the number of surface Ce atoms to the total number of Ce atoms without a more detailed knowledge of the structure of the nanoparticle, the ratio is clearly very large (20%–50%) for the 3.1 nm particles. It

is thus unclear whether the larger trivalent cerium atoms reside at the surface (which would be consistent with standard rare earth surface science) or in the core of the nanoparticle.

Application of Eq. (1) to our diffraction results showed that considerable lattice disorder (as represented by the strain percentage e) exists in the $CePt_2$ nanoparticles. Setting $e = 0$ for the bulk, we obtained $e = 0.02\%$ for $d =$ 22 nm and $e = 1.52\%$ for $d = 3.1$ nm. Large bond-length disorder was observed for $CePt_2$ and $CeAl_2$ nanocrystals through analysis of XAFS measurements [8]. The moderate decreases of T_K and T_N and the fraction n_{AF} of the AF contribution observed [12,13] in bulk $CePt_{2+x}$ ($x = 0$, 0.5, 1) alloys as the alloy parameter x increases are very similar to those observed in the 26 and 22 nm $CePt_2$ nanoparticles. For the alloys, these effects arise primarily from site disorder (Pt on Ce sites) suggesting that site and/or structural disorder may be responsible for these effects observed in the 26 and 22 nm nanocrystals of $CePt_2$.

Analysis of the XAFS [8] showed, however, that the small Kondo temperature of the trivalent magnetic fraction of the 3.1 nm particles cannot arise from bond-length disorder. One possibility is that the trivalent atoms are associated with defects in the $C15$ structure where the $4f$–conductance-electron hybridization is reduced; there might be considerably many such defect sites at small particle size. Another possibility is that the small Kondo temperature can be attributed to a quantum size effect of the sort discussed in recent theory [2,3,16].

According to the theoretical model of Thimm *et al.* [3] the Kondo resonance should be strongly affected when the mean conduction electron level spacing in the nanoparticle becomes larger than the Kondo temperature. According to Halperin [1], in a free-electron model the energy level spacing ξ is related to the average density of states (DOS) per spin at the Fermi surface. ξ is inversely proportional to d^3 and can be estimated from

$$\xi = \frac{(5.58\ \mathrm{nm})^3 \nu_m}{\gamma d^3}, \qquad (2)$$

where $\gamma(\mathrm{mJ/mol\,K^2})$ is the specific heat coefficient, and ν_m ($\mathrm{cm^3/mol}$) is the molar volume. Using the values $\gamma =$ 5–10 $\mathrm{mJ/mol\,K^2}$ for $LaPt_2$ given above, ξ is estimated to be 4.5–9, 0.1–0.2, and 0.06–0.12 K for $d = 3.1$, 22, and 26 nm, respectively. The electronic energy level spacing $\xi \sim 4.5$–9 K for a 3.1 nm particle is thus comparable or larger than either the Kondo temperature $T_K = 5.6$ K or the Néel temperature $T_N = 1.6$ K of bulk $CePt_2$. This lends further credence to our contention that the behavior of the trivalent fraction of 3.1 nm particles involves a quantum size effect. We note, however, that according to the theoretical work of Ref. [2], the specific heat should be exponentially activated at low T due to the discreteness of the energy spectrum. This should lead to a low value of specific heat, rather than the rather large values actually observed, which are most clearly visible on application of a magnetic field (Fig. 2 inset).

In conclusion, we have reported the suppression of magnetic correlations and the enhancement of Kondo interactions on particle size reduction in $CePt_2$ nanoparticles. Lattice disorder is probably the origin of the variations of Kondo interactions and magnetic order for the larger nanoparticles. At the smallest particle size, 3.1 nm, an increase in the background DOS is possibly responsible for the strong mixed valence in most of the sample. However, since the electronic energy level spacing ξ for the 3.1 nm particles is comparable or larger than T_K and T_N of bulk $CePt_2$, the large reduction of T_K of the trivalent fraction at ultrasmall particle size may well arise from a quantum size effect.

This work was supported by the National Science Council of the Republic of China under Grant No. NSC95-2120-M-001-004 and the Office of Basic Energy Sciences, U. S. Department of Energy under Contract No. AC03-76SF00098.

*Electronic address: cheny2@phys.sinica.edu.tw
†Present address: Department of Materials Engineering, Tatung University, Taipei, Taiwan, Republic of China.

[1] W. P. Halperin, Rev. Mod. Phys. **58**, 533 (1986).
[2] P. Schlottman, Phys. Rev. B **65**, 174407 (2002).
[3] W. B. Thimm, J. Kroha, and J. V. Delft, Phys. Rev. Lett. **82**, 2143 (1999).
[4] T. W. Odom, J.-L. Huang, C. L. Cheung, and C. M. Lieber, Science **290**, 1549 (2000).
[5] V. Madhavan, W. Chen, T. Jamneala, M. F. Crommie, and N. S. Wingreen, Science **280**, 567 (1998).
[6] C. H. Booth, M. D. Walter, M. Daniel, W. W. Lukens, and R. E. Anderson, Phys. Rev. Lett. **95**, 267202 (2005).
[7] Y. Y. Chen, Y. D. Yao, C. R. Wang, W. H. Li, C. L. Chang, T. K. Lee, T. M. Homg, J. C. Ho, and S. F. Pan, Phys. Rev. Lett. **84**, 4990 (2000).
[8] S.-W. Han, C. H. Booth, E. D. Bauer, P. H. Huang, Y. Y. Chen, and J. M. Lawrence, Phys. Rev. Lett. **97**, 097204 (2006).
[9] C. Verdozzi, Y. Luo, and N. Kioussis, Phys. Rev. B **70**, 132404 (2004).
[10] I. K. Yanson, V. V. Fisun, R. Hesper, A. V. Khotkevich, J. M. Krans, J. A. Mydosh, and J. M. van Ruitenbeek, Phys. Rev. Lett. **74**, 302 (1995).
[11] R. R. Joseph, K. A. Gschneidner, Jr., and R. F. Hungsberg, Phys. Rev. B **5**, 1878 (1972).
[12] J. M. Lawrence, Y. C. Chen, G. H. Kwei, M. F. Hundley, and J. D. Thompson, Phys. Rev. B **56**, 5 (1997).
[13] Y. Y. Chen, P. H. Huang, C. H. Booth, and J. M. Lawrence, Physica (Amsterdam) **B378–380**, 778 (2006).
[14] A. J. C. Wilson, Proc. Phys. Soc. London **81**, 41 (1963).
[15] P. D. Sacramenrto and P. Schlottmann, Phys. Rev. B **40**, 431 (1989).
[16] The field dependence of the specific heat (Fig. 2, inset) has some similarity to that expected for a spin glass compound; e.g., see K. Binder and A. P. Young, Rev. Mod. Phys. **58**, 801 (1986). Spin glass behavior, however, would also require trivalent Ce atoms, with vanishingly small TK. Our discussion of the origin of the trivalence remains unaltered for this case.